

Supporting information for :

Discrimination of 4-Hydroxyproline Diastereomers by Vibrational Spectroscopy of the Gaseous Protonated Species

Maria Elisa Crestoni,^{*,†} Barbara Chiavarino,[‡] Debora Scuderi,[§] Annito Di Marzio,[‡] Simonetta Fornarini[‡]

[†] Dipartimento di Chimica e Tecnologie del Farmaco, Università di Roma ‘‘La Sapienza’’, P. le A. Moro 5, I-00185 Roma, Italy

[§] Laboratoire de Chimie Physique d’Orsay, Université Paris-Sud 11, Batiment 350-Campus d’Orsay 15, avenue Jean Perrin –91405 Orsay Cedex, France

Contents :

Figure 1S. Relative abundances of mass selected (a) HypH⁺ and (b) hypH⁺ ions (■, m/z 132) and of daughter ion (▲, m/z 86) as a function of collision energy (E_{CM}/eV).

Figure 2S. Photodissociation mass spectrum of protonated (2S,4R)-4-hydroxyproline (HypH⁺) ions at m/z 132 before (a) and after (b) irradiation with OPO/OPA IR frequency fixed at 3550 cm⁻¹.

Figure 3S. Photodissociation mass spectrum of protonated (2S,4S)-4-hydroxyproline (hypH⁺) ions at m/z 132 before (a) and after (b) irradiation with CLIO FEL IR frequency fixed at 1770 cm⁻¹.

Figure 4S. Optimized structures and relative free energies (in parentheses) at 298 K (kJ mol⁻¹) of protonated (2S,4R)-4-hydroxyproline (HypH⁺) conformers **R**-_{endo} **Ic**, **R**-_{exo} **IIIa**, **R**-_{exo} **IIIb**, **R**-_{endo} **IIa**, **R**-_{endo} **IIc**, **R**-_{endo} **IIIa**, **R**-_{endo} **IIIc**, calculated at MP2/6-311+G** level of theory.

Figure 5S. Optimized structures and relative free energies (in parentheses) at 298 K (kJ mol⁻¹) of hypH⁺ conformers **S**-_{endo} **Ic**, **S**-_{exo} **Ic**, **S**-_{endo} **IIIa**, **S**-_{exo} **IIa**, **S**-_{endo} **IIIb**, **S**-_{exo} **IIc**, **S**-_{exo} **IIIa**, **S**-_{endo} **IIIc**, **S**-_{exo} **IIIc**, calculated at MP2/6-311+G** level of theory. Hydrogen bond lengths, marked by dashed lines, are given in Å.

Figure 6S. Calculated IR spectra of protonated (2S,4R)-4-hydroxyproline (HypH⁺) structures **R**-_{endo} **Ic**, **R**-_{exo} **IIIa**, **R**-_{exo} **IIIb**, **R**-_{endo} **IIa**, at the MP2/6-311+G** level.

Figure 7S. Calculated IR spectra of protonated (2S,4R)-4-hydroxyproline (HypH^+) structures **R-_{endo} IIc**, **R-_{endo} IIIa**, **R-_{endo} IIIc** at the MP2/6-311+G** level.

Figure 8S. Calculated IR spectra of protonated (2S,4S)-4-hydroxyproline (hypH^+) structures **S-_{endo} Ic**, **S-_{exo} Ic**, **S-_{endo} IIIa**, **S-_{exo} IIa**, **S-_{endo} IIIb** at the MP2/6-311+G** level.

Figure 9S. Calculated IR spectra of protonated (2S,4S)-4-hydroxyproline (hypH^+) structures **S-_{exo} IIc**, **S-_{exo} IIIa**, **S-_{endo} IIIc**, **S-_{exo} IIIc** at the MP2/6-311+G** level.

Figure 10S. Experimental IRMPD spectra of protonated (2S,4R)-4-hydroxyproline (HypH^+) enlarged in the higher frequency OH stretch region, showing all data points.

Figure 11S. Experimental IRMPD spectra of protonated (2S,4S)-4-hydroxyproline (hypH^+) enlarged in the higher frequency OH stretch region, showing all data points.

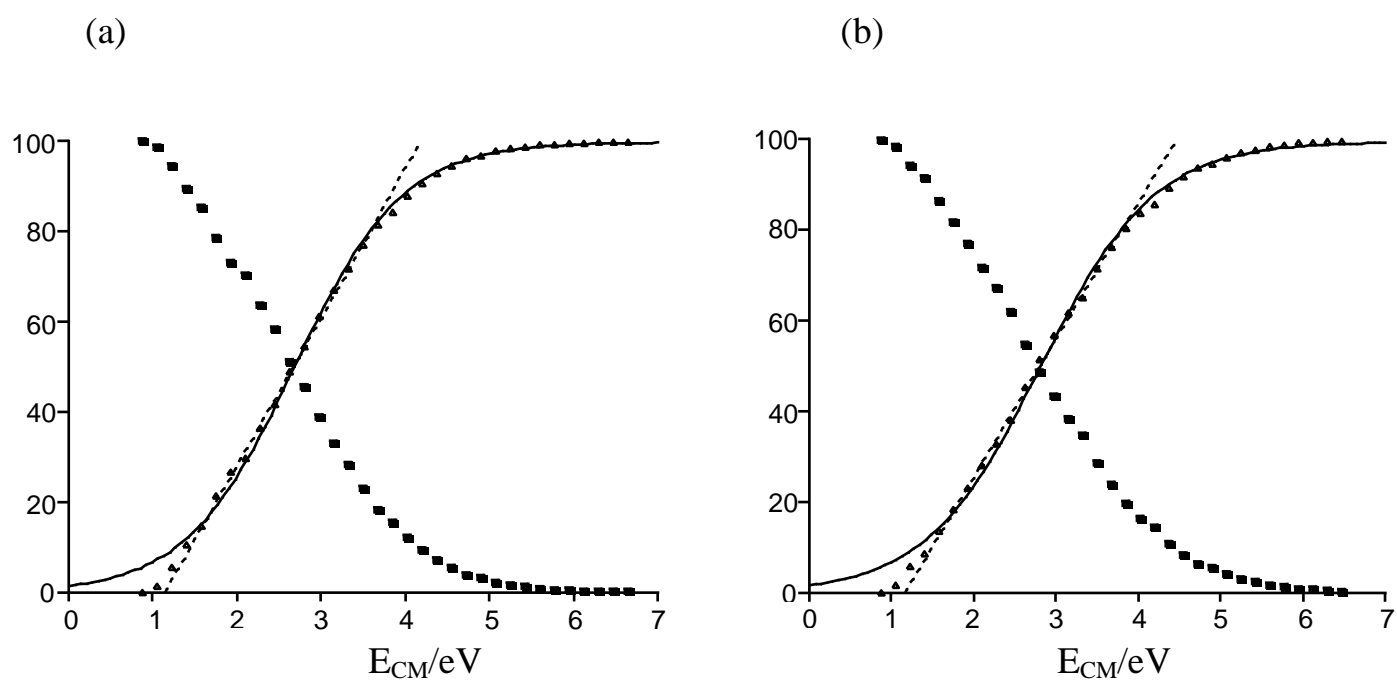


Figure 1S. Relative abundances of mass selected (a) HypH+ and (b) hypH+ ions (■, m/z 132) to afford daughter ion (▲, m/z 86) as a function of collision energy (center of mass, E_{CM}/eV).

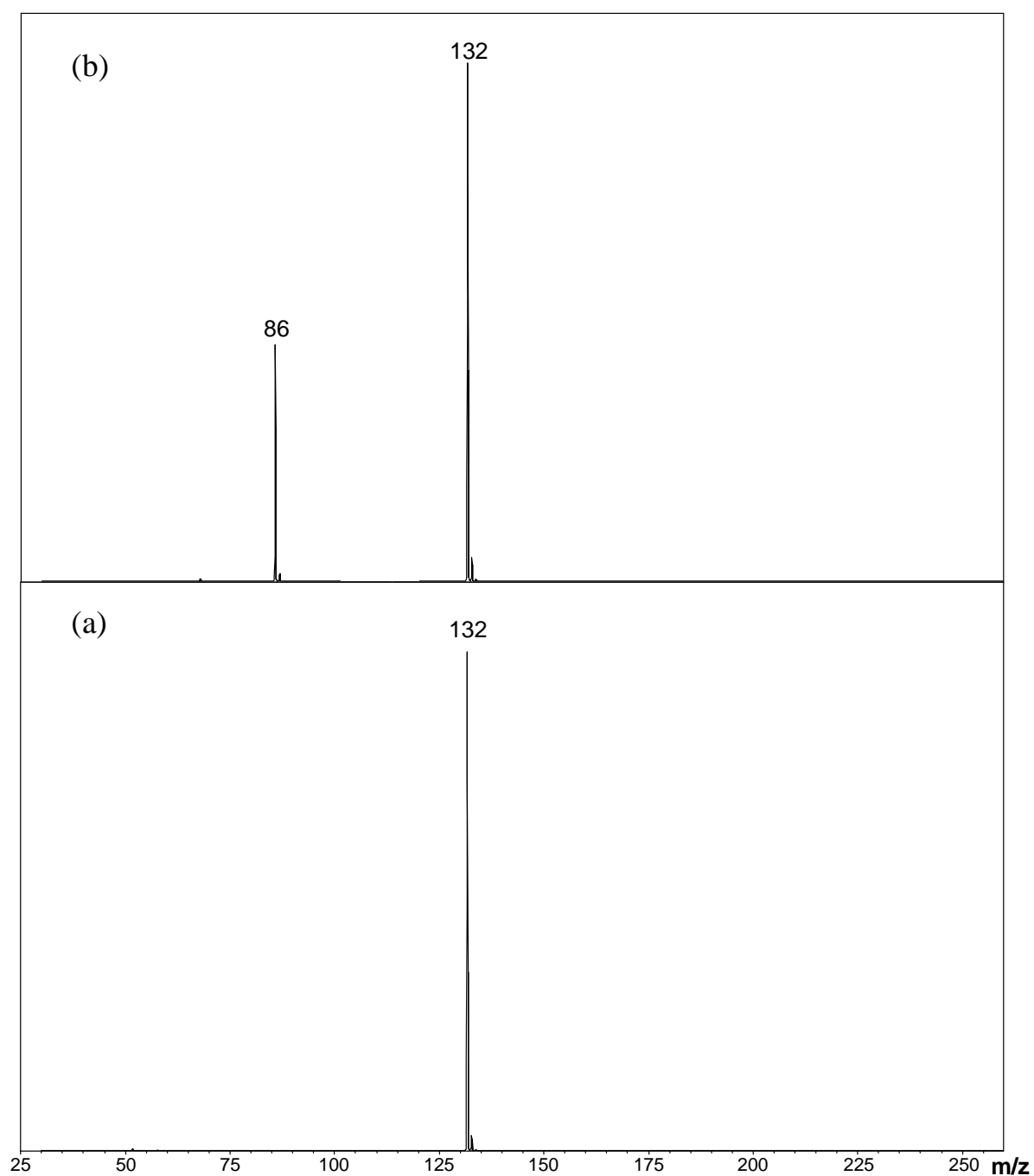


Figure 2S. Photodissociation mass spectrum of protonated (2S,4R)-4-hydroxyproline (HypH^+) ions at m/z 132 before (a) and after (b) irradiation with OPO/OPA IR frequency fixed at 3550 cm^{-1} .

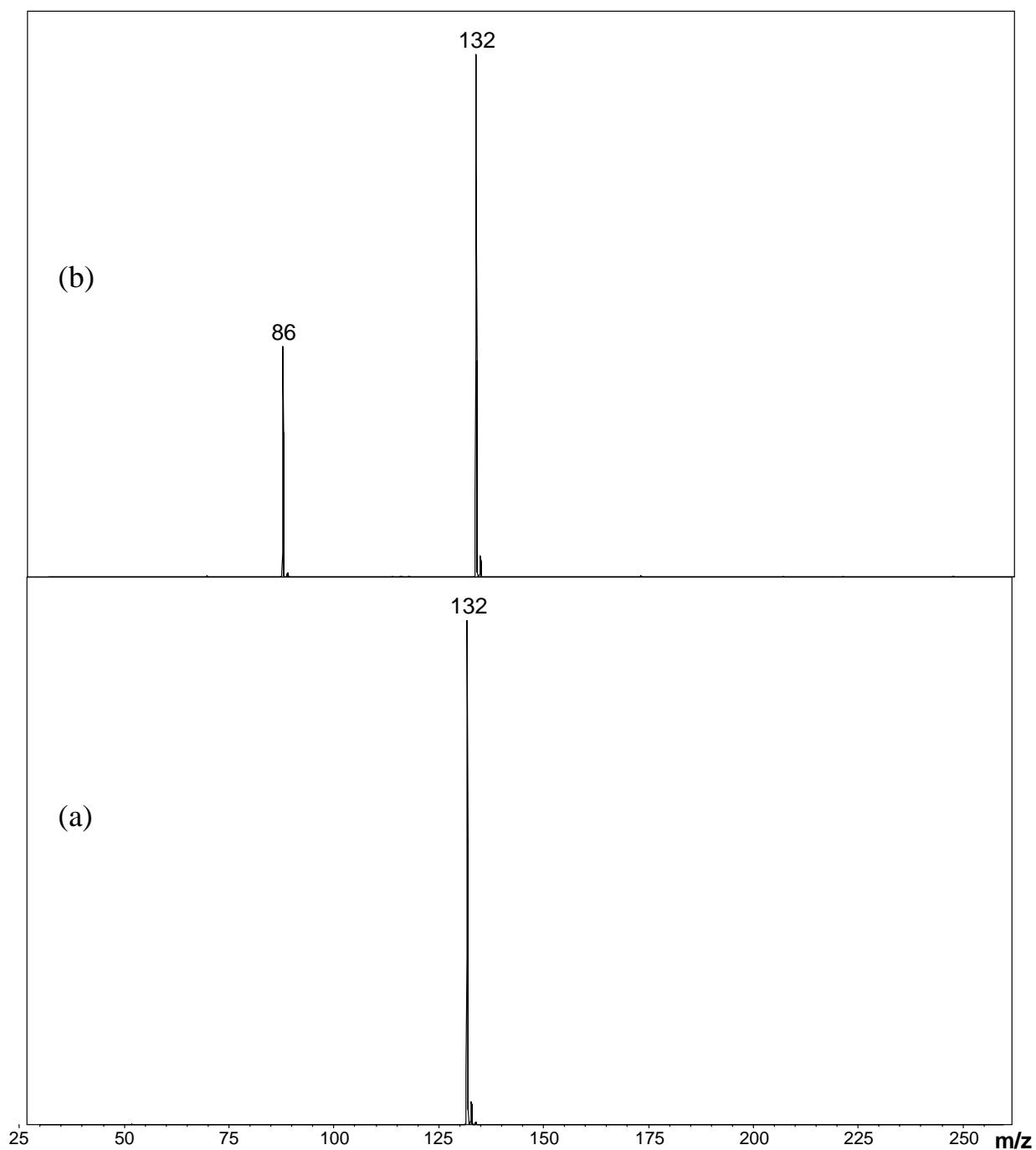
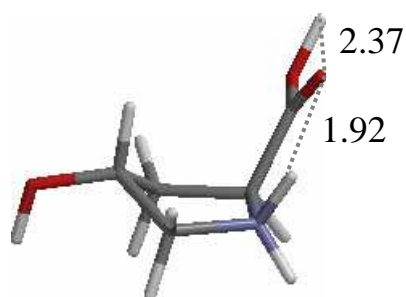
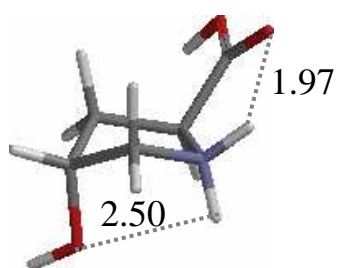


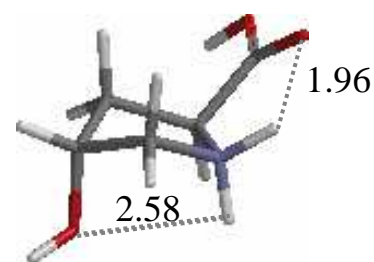
Figure 3S. Photodissociation mass spectrum of protonated (2S,4S)-4-hydroxyproline (hypH^+) ions at m/z 132 before (a) and after (b) irradiation with CLIO FEL IR frequency fixed at 1770 cm^{-1} .



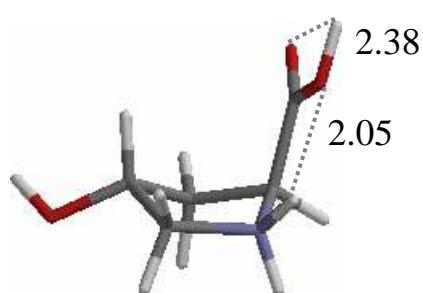
R-endo Ic (33.6)



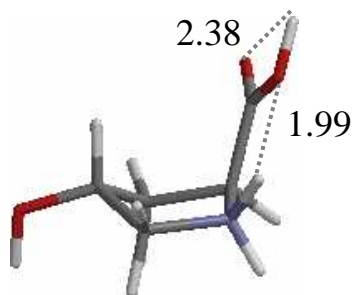
R-exo IIIa (34.8)



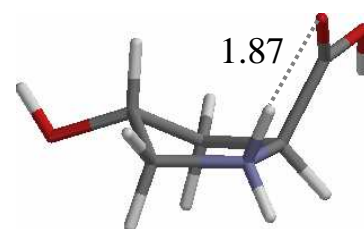
R-exo IIIb (35.2)



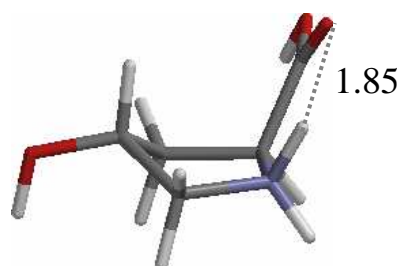
R-endo IIa (37.4)



R-endo IIc (51.1)



R-endo IIIa (55.5)



R-endo IIIc (69.1)

Figure 4S. Optimized structures and relative free energies (kJ mol^{-1} , in parentheses) at 298 K of protonated (2S,4R)-4-hydroxyproline (HypH^+) conformers **R-endo Ic**, **R-exo IIIa**, **R-exo IIIb**, **R-endo IIa**, **R-endo IIc**, **R-endo IIIa**, **R-endo IIIc**, calculated at MP2/6-311+G** level of theory.

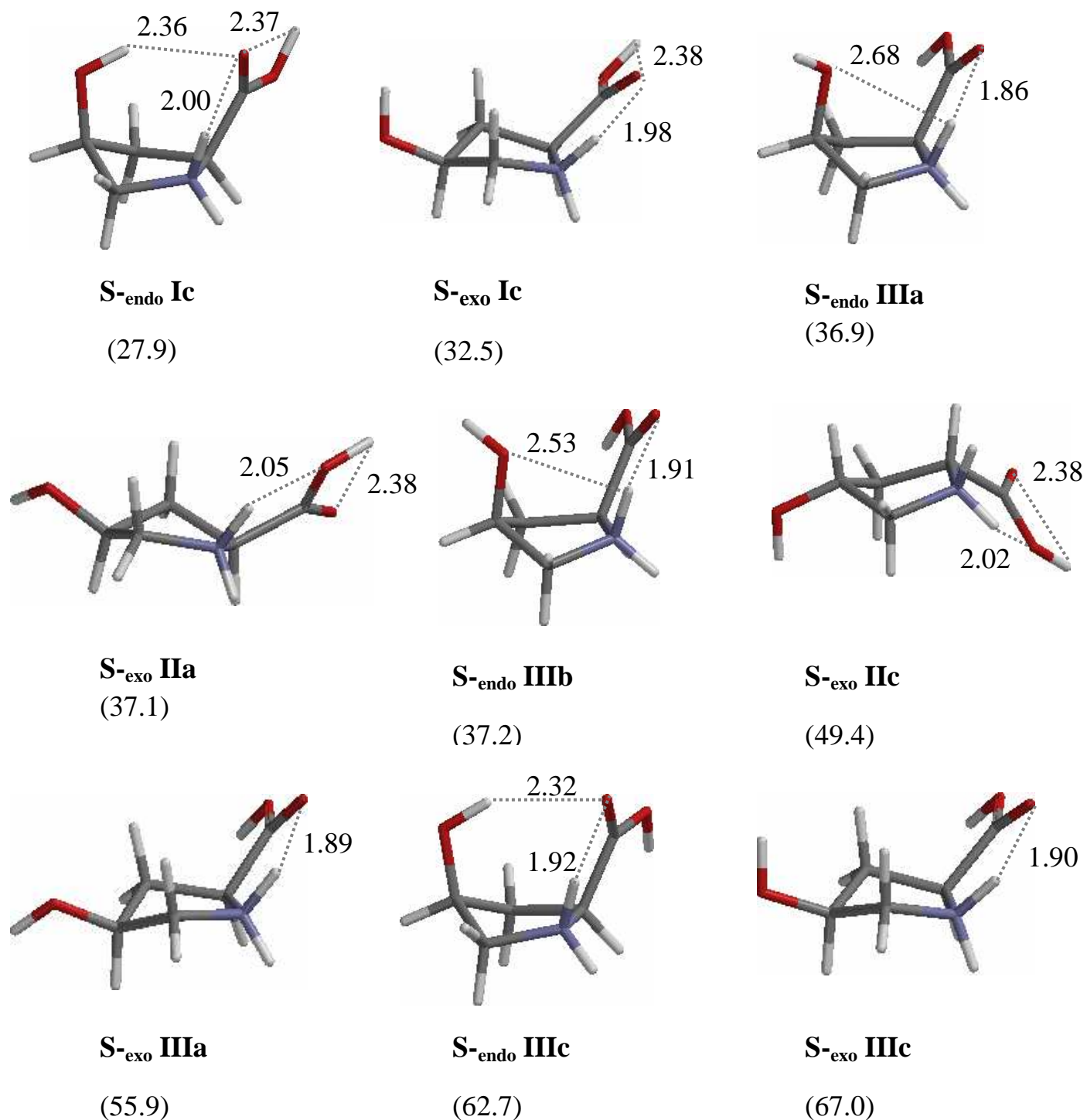


Figure 5S. Optimized structures and relative free energies (kJ mol⁻¹, in parentheses) at 298 K of hypH⁺ conformers **S-_{endo} Ic**, **S-_{exo} Ic**, **S-_{endo} IIIa**, **S-_{exo} IIa**, **S-_{endo} IIIb**, **S-_{exo} IIc**, **S-_{exo} IIIa**, **S-_{endo} IIIc**, **S-_{exo} IIIc**, calculated at MP2/6-311+G** level of theory. Hydrogen bond lengths, marked by dashed lines, are given in Å.

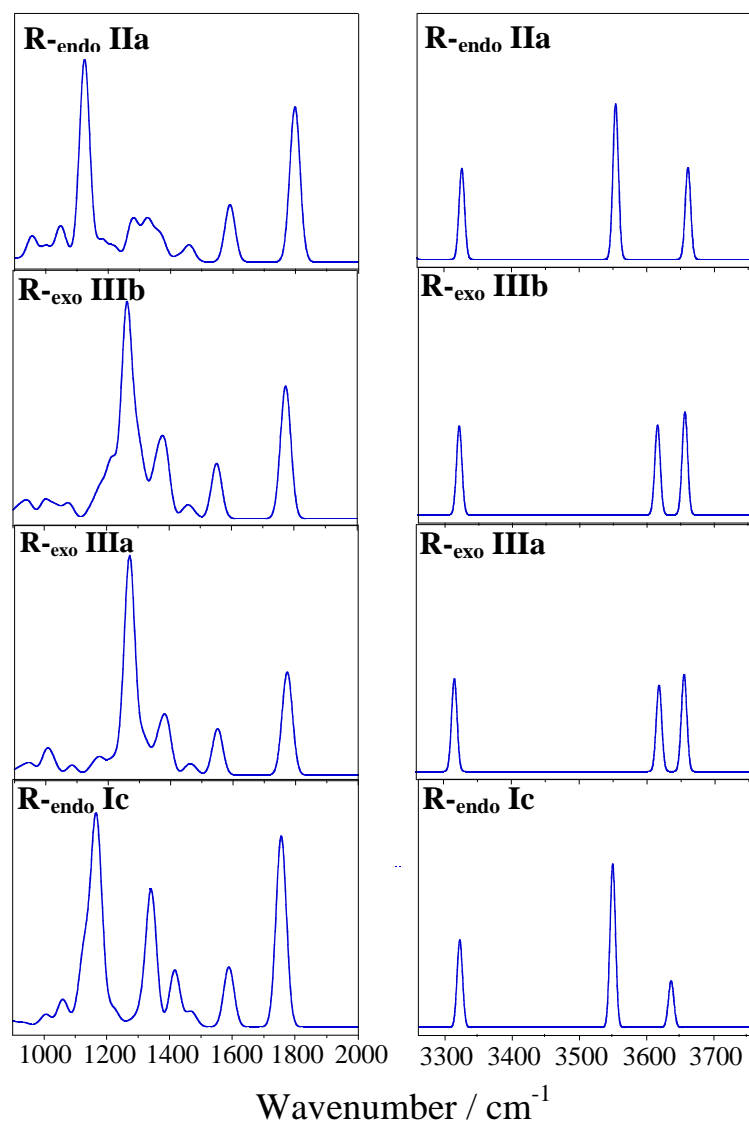


Figure 6S. Calculated IR spectra of protonated (2S,4R)-4-hydroxyproline (HypH⁺) structures **R-endo Ic**, **R-exo IIIa**, **R-exo IIIb**, **R-endo IIa**, at the MP2/6-311+G** level.

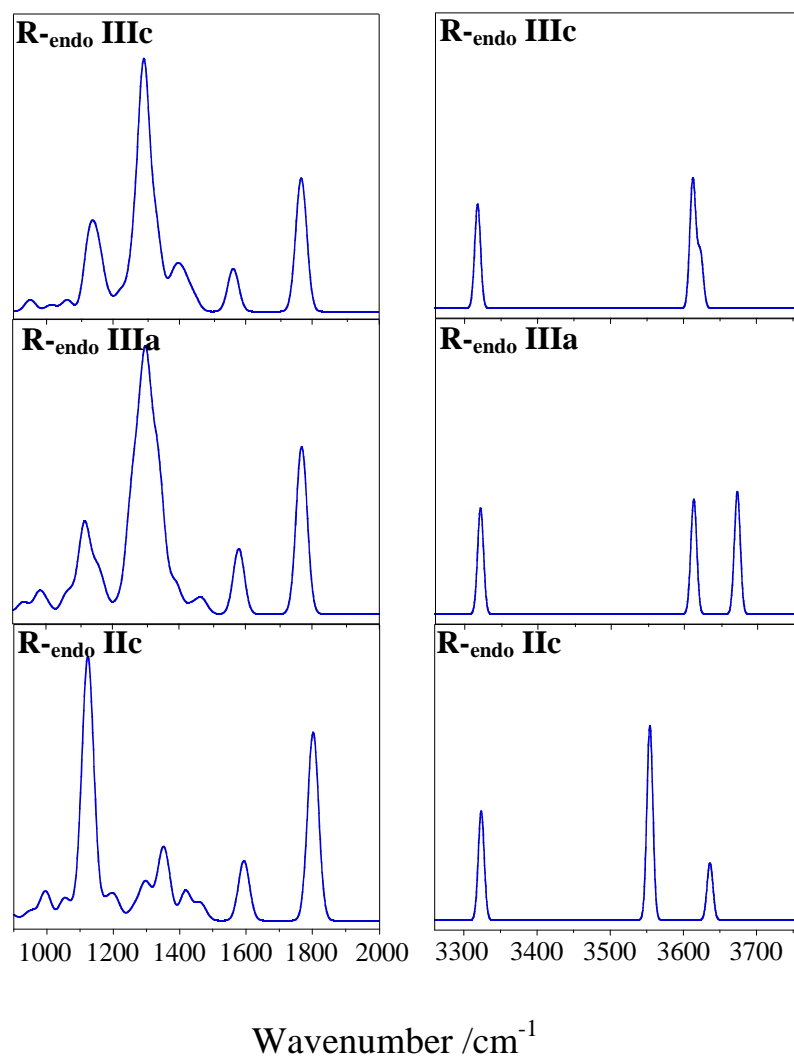


Figure 7S. Calculated IR spectra of protonated (2S,4R)-4-hydroxyproline (HypH⁺) structures **R-endo IIc**, **R-endo IIIa**, **R-endo IIIc** at the MP2/6-311+G** level.

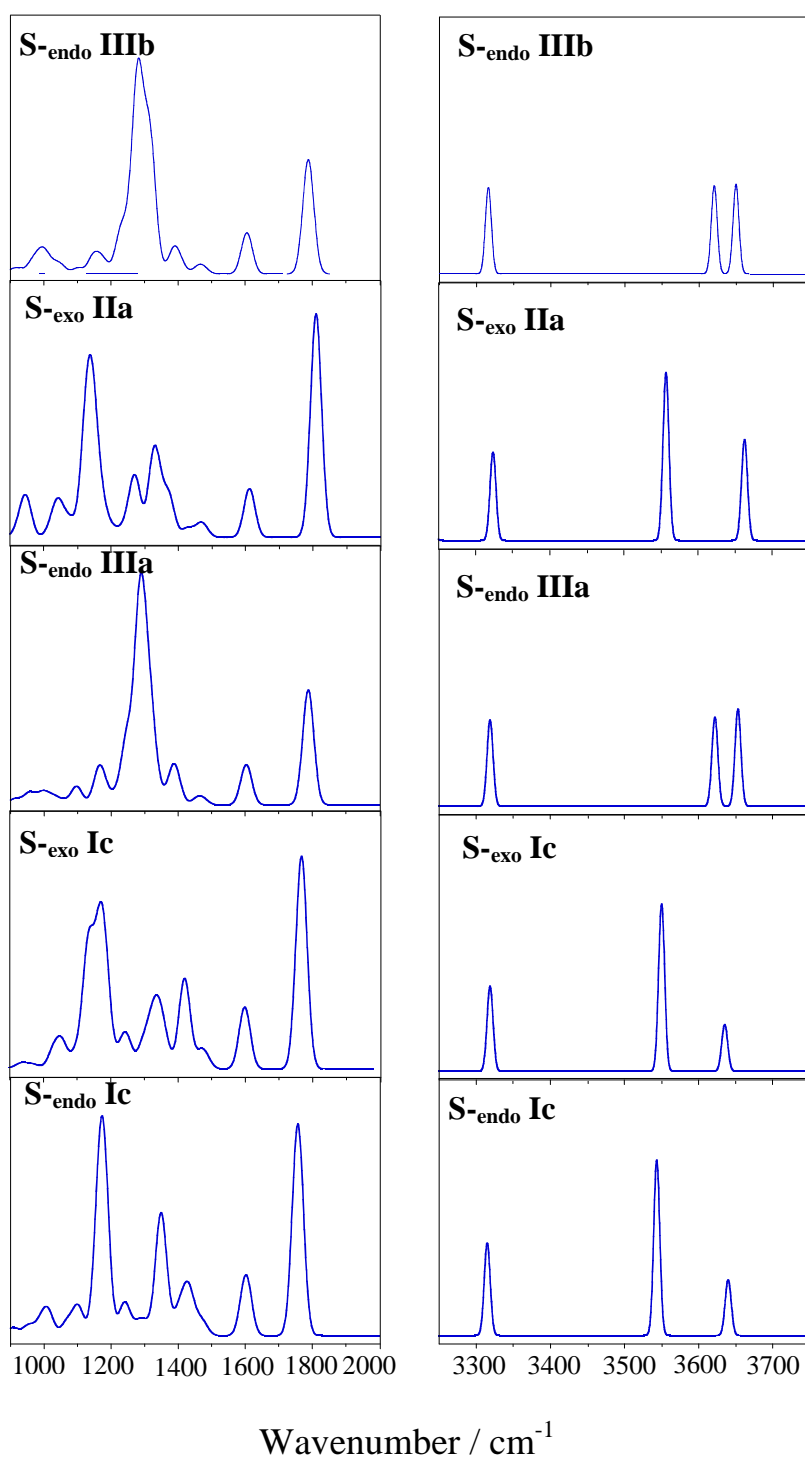


Figure 8S. Calculated IR spectra of protonated (2S,4S)-4-hydroxyproline (hypH⁺) structures **S-endo Ic**, **S-exo Ic**, **S-endo IIIa**, **S-exo IIa**, **S-endo IIIb** at the MP2/6-311+G** level.

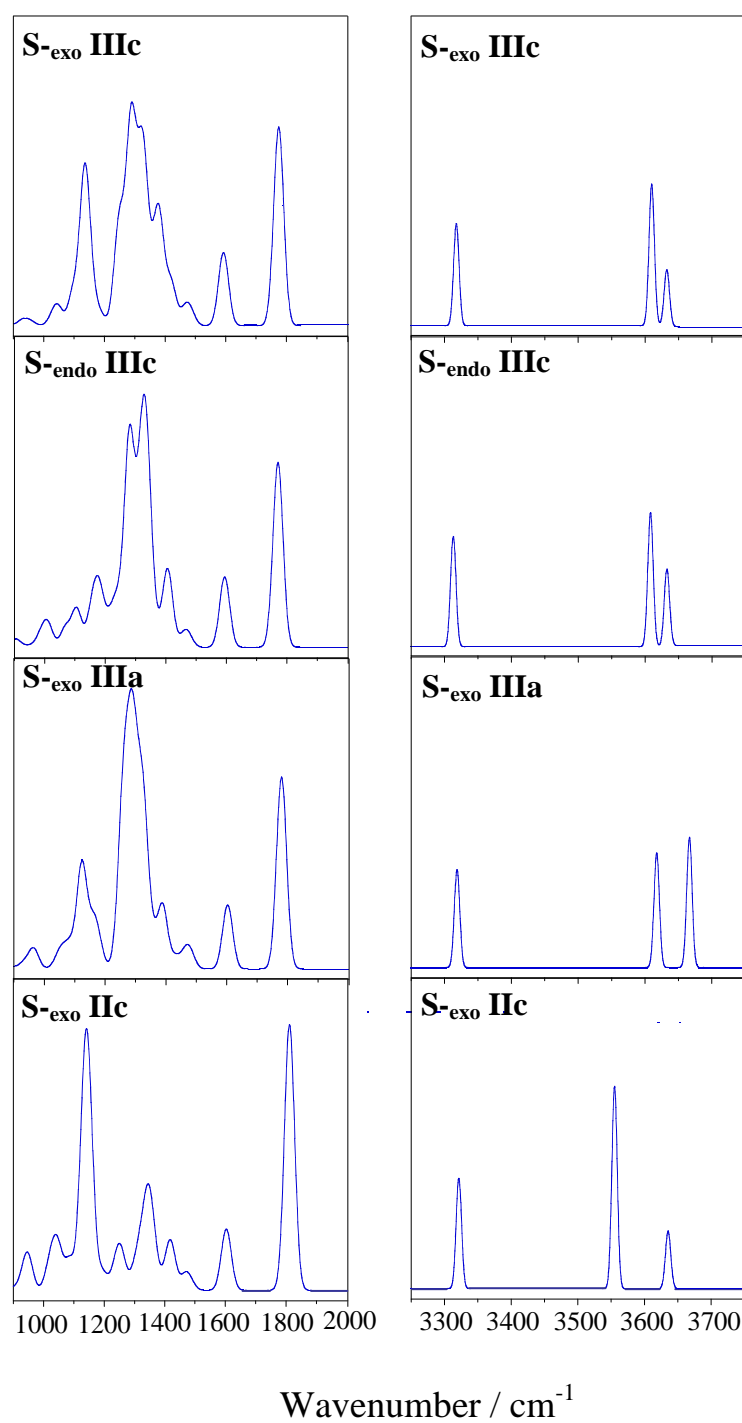


Figure 9S. Calculated IR spectra of protonated (2S,4S)-4-hydroxyproline (hypH⁺) structures **S-exo IIc**, **S-exo IIIa**, **S-endo IIIc**, **S-exo IIIc** at the MP2/6-311+G** level.

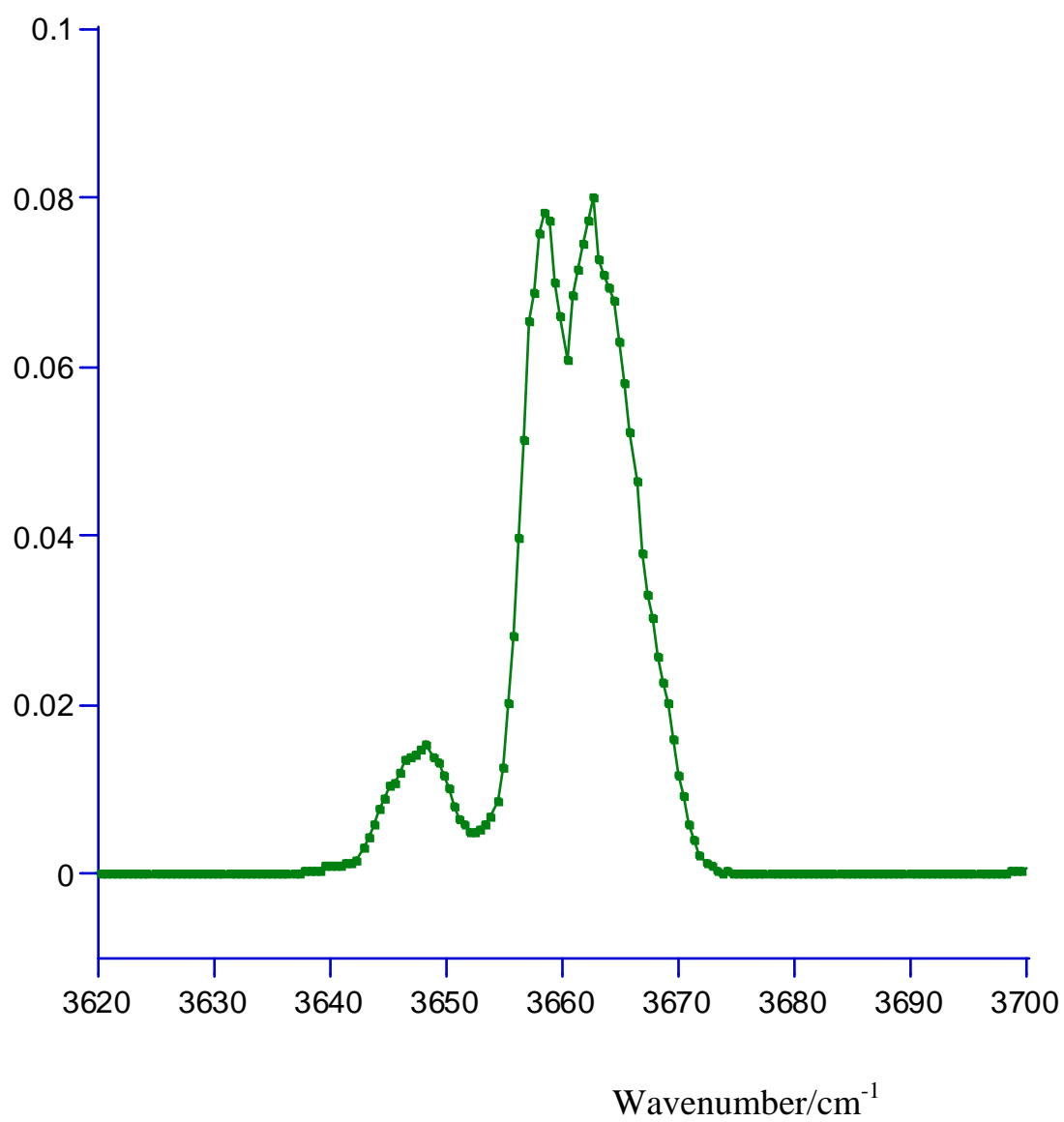


Figure 10S. Experimental IRMPD spectra of protonated (2S,4R)-4-hydroxyproline (HypH⁺) enlarged in the higher frequency OH stretch region, showing all data points.

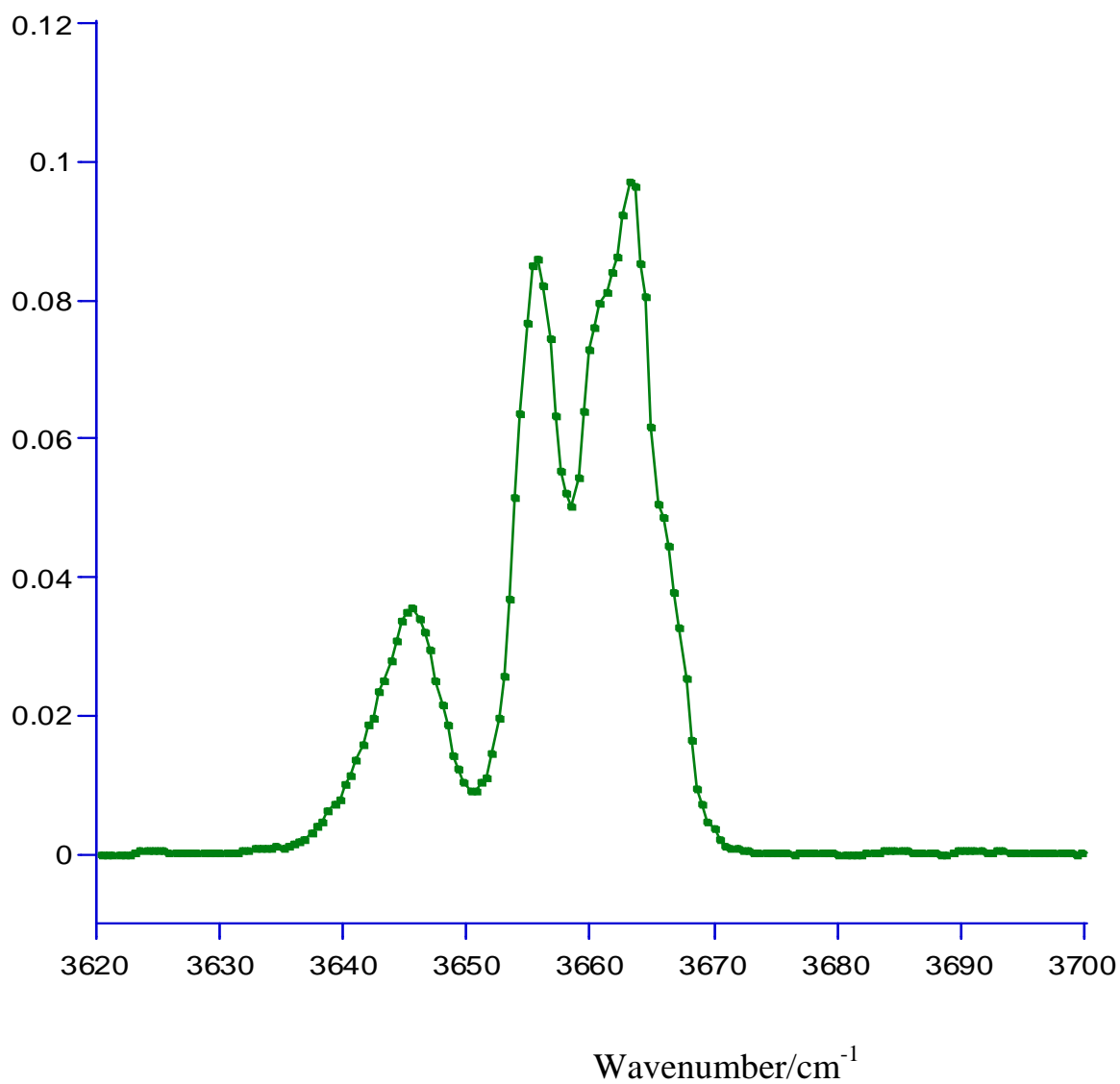


Figure 11S. Experimental IRMPD spectra of protonated (2S,4S)-4-hydroxyproline (hypH⁺) enlarged in the higher frequency OH stretch region, showing all data points.